Frontiers of Optoelectronics (2022) 15:30
https://doi.org/10.1007/s12200-022-00034-3

Frontiers of Optoelectronics

RESEARCH ARTICLE

N-doped carbon anchored CoS_2/MoS_2 nanosheets as efficient electrocatalysts for overall water splitting

Xingwei Zhou[1] · Wei Zhang[1,2] · Zunhao Zhang[1] · Zizhun Wang[1] · Xu Zou[1] · Dabing Li[3] · Weitao Zheng[1]

Received: 12 April 2022 / Accepted: 9 May 2022

Abstract
The oriented two-dimensional porous nitrogen-doped carbon embedded with CoS_2 and MoS_2 nanosheets is a highly efficient bifunctional electrocatalyst. The hierarchical structure ensures fast mass transfer capacity in improving the electrocatalytic activity. And the greatly increased specific surface area is beneficial to expose more electrocatalytically active atoms. For oxygen evolution reaction (OER) and hydrogen evolution reaction (HER) tests in 1 mol/L KOH solution, only 194 and 140 mV overpotential are required to achieve a current density of 10 mA/cm^2, respectively. Our research provides an effective strategy for synergizing the individual components in nanostructures for a wide range of electrocatalytic reactions.

Keywords Oxygen evolution reaction · Hydrogen evolution reaction · Bifunctional electrocatalyst · Overall water splitting

1 Introduction

Electrochemical water splitting ensures green and safe conversion of electrical energy to chemical energy [1–4]. However, water splitting is a thermodynamically uphill process and thus needs to be modulated by efficient hydrogen and oxygen evolution catalysts simultaneously to lower the reaction energy barrier. Noble metal-based electrocatalysts have been widely explored by reducing the activation energy barrier of the reaction and improving the energy conversion efficiency [5]. However, limited resources and expensiveness of these precious metals, severely hamper their large-scale applications. Transition metals and their compounds have attracted much attention, as they are abundant on earth, and offer excellent electrochemical properties [6–9]. A large number of such noble-metal-free materials have been synthesized but are electrocatalytically active for hydrogen evolution reaction (HER) or oxygen evolution reaction (OER) only. In contrast, bifunctional electrocatalysts that are effective for both HER and OER are more advantageous for overall water splitting, but are less common. A bifunctional electrocatalyst can be more easily integrated into a single water splitting device, and the HER and OER performances of the electrocatalyst can be optimized simultaneously.

It is well known that the number of active sites is critical to the overall activity of electrocatalysts. These active sites usually appear at the surfaces, including steps, kinks and edges of nanoscale structures [10]. In recent years, molybdenum disulfide (MoS_2) has received extensive attention. Theoretical studies have shown that the MoS_2 edge atoms exhibit excellent catalytic activity, while the basal plane atoms are chemically inert. One approach is to activate the basal plane of inert atoms and reduce the band gap by doping transition metal atoms (e.g., Ni, Co, Fe, Zn, and Ru) and non-metal atoms (e.g., C, N, O, P, and Se), thus improving their electrocatalytic properties [11, 12]. The exotic atoms can produce a local electron density at the host atoms, which can modify the energy barrier of the reaction by breaking the periodicity of MoS_2. Another way to increase the quantity of active sites

✉ Wei Zhang
weizhang@jlu.edu.cn

✉ Xu Zou
zoux@jlu.edu.cn

1 Key Laboratory of Automobile Materials MOE, School of Materials Science and Engineering, Electron Microscopy Center, and International Center of Future Science, Jilin Provincial International Cooperation Key Laboratory of High-Efficiency Clean Energy Materials, Jilin University, Changchun 130012, China

2 Wuhan National Laboratory for Optoelectronics, Huazhong University of Science and Technology, Wuhan 430074, China

3 State Key Laboratory of Luminescence and Applications, Changchun Institute of Optics, Fine Mechanics and Physics, Chinese Academy of Sciences, Changchun 130033, China

Published online: 18 July 2022

of MoS_2 is to increase the density of the edge atoms by constructing specific nanostructures [13, 14]. Besides, the catalytic activity of the inert atoms in the 2H-MoS_2 basal plane can be enhanced by coupling with the conducting substrate (e.g., carbon cloth, nickel foam) [15].

Metal organic framework (MOF) is gradually becoming a new class of crystalline materials, which has attracted much attention due to its porosity, high specific surface and controllable properties [16–19]. These advantages ensure a high mass transfer capacity and a wealth of active sites, which are beneficial to the improvement of electrocatalytic activity. Besides, constructing electrocatalysts with rich hierarchical structures helps to improve the overall activity of electrocatalysts [20].

In this work, a bifunctional electrocatalyst MoS_2/CoS_2/carbon cloth (MOS/COS/CC) was prepared by embedding both CoS_2 and MoS_2 nanosheets in the oriented 2D porous N-doped carbon nanosheets. The porous structure of N-doped carbon nanosheets embedded with CoS_2 nanosheets has positive effect on electrocatalytic activity. The introduction of MoS_2 nanosheets greatly increases the specific surface area of the material, which is beneficial to the exposure of electrocatalytic active sites. Compared with use of powder electrocatalysts, employment of carbon cloth as the substrate greatly improves the conductivity and mechanical flexibility of the electrode. The interaction of the porous N-doped carbon nanosheets embedded with CoS_2 and MoS_2 nanosheets leads to the excellent performance of the bifunctional electrocatalysts. Testing the OER and HER performances of MOS/COS/CC in 1 mol/L KOH solution requires only an overpotential of 194 and 140 mV, respectively, to reach a current density of 10 mA/cm^2. Our study provides an effective strategy for the construction of nanostructured bifunctional electrocatalysts.

2 Experiment

2.1 Chemicals and reagents

Cobalt nitrate hexahydrate ($Co(NO_3)_2{\cdot}6H_2O$), 2-methylimidazole ($C_4H_6N_2$), platinum on carbon (20% Pt/C) and ruthenium (IV) oxide (RuO_2) were purchased from Aladdin Chemistry Co., Ltd. Ethanol (CH_3CH_2OH), thiourea (CH_4N_2S), sodium molybdenum oxide ($MoNa_2O_4$) and hydroxyacetone ($C_3H_6O_2$) were purchased from Sinopharm Chemical Reagent Co., Ltd. Carbon cloth was purchased from CeTech Co., Ltd. Highly purified water (> 18 MΩ·cm resistivity) was obtained from a PALL PURELAB Plus system.

2.2 Synthesis of MOS/COS/CC

The synthesis process of the MOS/COS/CC electrocatalyst is represented in Fig. 1. First, the synthesis of MOF-CC was carried out using a solution route. $Co(NO_3)_2{\cdot}\ 6H_2O$ (582 mg) and $C_4H_6N_2$ (1.3 g) were dissolved in 25 mL of deionized water and recorded as A and B solutions, respectively. Then, after magnetic stirring for 0.5 h, solution A was quickly poured into solution B. The carbon cloth was placed in the obtained mixed solution and kept at room temperature for 4 h to obtain MOF-CC. Then, the MOF-CC was annealed in a tube furnace at 750 °C for 2 h. The heating rate was set as 5 °C/min. In the next step, CH_4N_2S (609 mg) was mixed with 30 mL of ionized water and stirred for 10 min. $MoNa_2O_4$ (483.9 mg) was added to the above solution and stirred for 30 min. The annealed sample was put into the mixed solution that was then placed in a reactor. The reactor was heated to 200 °C and maintained at that temperature for 2, 4, 6, and 8 h respectively to obtain four different samples. After hydrothermal reaction, MoS_2 nanosheets were deposited on MOF-CC. A bifunctional electrocatalyst containing 2D porous N-doped nanosheets embedded with CoS_2 and MoS_2 nanosheets (MOS/COS/CC) was thus prepared.

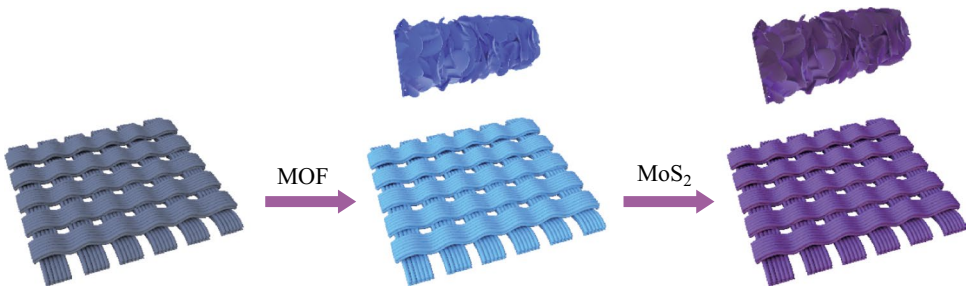

Fig. 1 Schematic illustration of MOS/COS/CC electrocatalyst synthesis process

2.3 Electrochemical measurements

In the OER and HER tests, self-supporting catalysts were used as working electrodes. A graphite rod and saturated calomel (saturated KCl solution) electrodes were used as counter and reference electrodes, respectively. All potentials were converted to reversible hydrogen potentials. The Tafel slope was calculated by

$$\eta = a + b \log |j|,$$

where η is the overvoltage, b is the Tafel slope and j is the current density. The catalyst ink (5 mg/mL) was prepared by dispersing 5 mg of the catalyst into 1 mL of solution containing 0.73 mL of ultrapure water, 0.25 mL of absolute ethanol and 10 μL of Nafion (5%), followed by ultrasonication treatment for 0.5 h. Then 10 μL of the catalyst ink was deposited on the glassy carbon electrode (GCE) with loading of 0.25 mg/cm^2. Linear sweep voltammetry (LSV)tests of OER and HER were performed at a scan rate of 5 mV/s in a solution of 1.0 mol/L KOH at room temperature, and the compensation potential was corrected by electrochemical impedance spectroscopy.

2.4 Characterization

X-ray diffraction (XRD) analysis was conducted using a Bruker D8 with Cu Kα irradiation. Scanning electron microscopy (SEM, Hitachi SU8010) was employed for morphology analysis. Transmission electron microscopic (TEM) and high-resolution TEM (HRTEM) images were recorded using an electron microscope (JEM-2100F). The energy dispersive X-ray spectroscopy (EDS) was performed in scanning transmission electron microscopy (STEM). Surface chemical states of the catalysts were detected by using an X-ray photoelectron spectroscope (XPS, ESCALAB-250).

3 Results and discussion

The heterostructure of MoS_2 and CoS_2 can be adjusted by controlling the growth time of MoS_2, which has a significant effect on the performance of the electrocatalysts. Electrocatalysts with growth times of 2, 4, 6, and 8 h were investigated. These samples were recorded as MOS/COS/CC-2 h, MOS/COS/CC-4 h, MOS/COS/CC-6 h and MOS/COS/CC-8 h, respectively. As shown in Fig. 2, the number of MoS_2 nanosheets deposited on the substrate increased with the growth time. As can be seen from Fig. 2a and e, the electrocatalysts with a deposition time of 2 h have a relatively small amount of MoS_2 nanosheets growing on the substrate. Due to the low surface area, the active sites in MOS/COS/CC-2 h are less exposed. This did not support improvement of the catalytic activity of the electrocatalyst. Figure 2d and h show that the leaf-like nitrogen-doped nanosheets had been covered up and the cracks had appeared in the electrocatalyst due to the long growth time, which had a fatal influence on the performance and stability of the electrocatalyst. For Fig. 2f and g, the MoS_2 nanosheets with a deposition time of 4 h and 6 h were the most impressive. The specific surface areas and number of active sites of MoS_2 nanosheets were much larger than other samples.

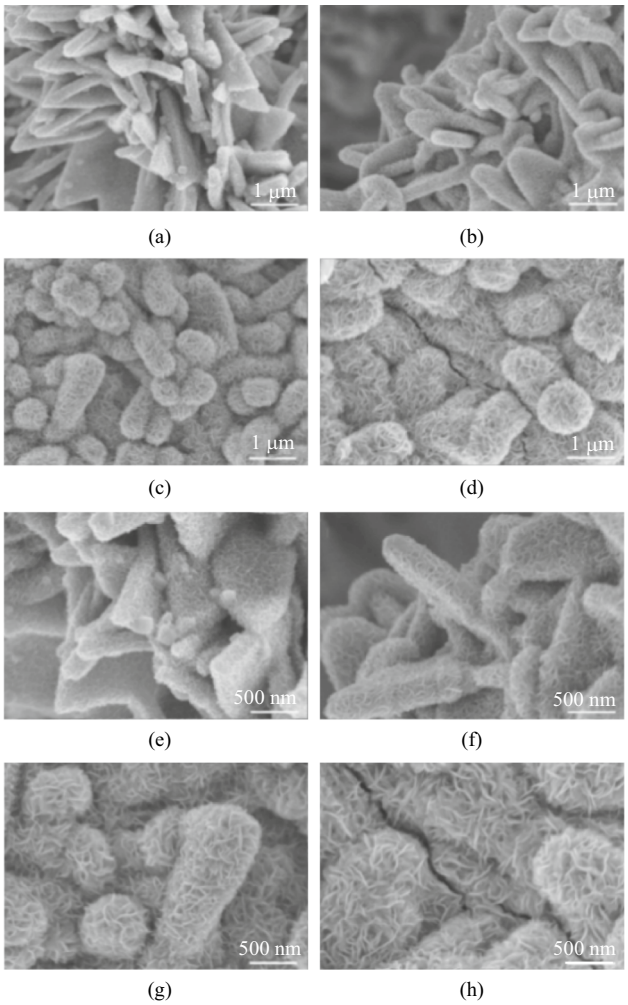

Fig. 2 SEM images of MOS/COS/CC electrocatalysts with different synthesis time. **a**, **e** 2 h, **b**, **f** 4 h, **c**, **g** 6 h, and **d**, **h** 8 h

Figure 3 shows the XRD pattern of the MOS/COS/CC electrocatalyst. The XRD patterns of MOS/COS/CC electrocatalysts show diffraction peaks at 32.6° (100), 39.8° (103) and 58.3° (110), which are in good agreement with those of MoS_2 in hexagonal 2H phase (PDF#37-1492). The diffraction angles of 27.8°, 32.3° and 36.2° correspond to the (111), (200) and (210) planes of CoS_2 (PDF#41-1471), respectively. Figure 4a and b show that the interplanar spacing of

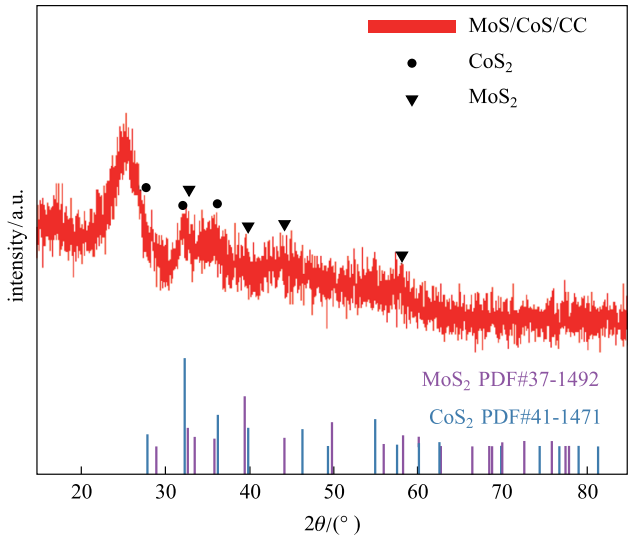

Fig. 3 XRD patterns of MoS/CoS/CC electrocatalysts

the layered structure is 0.65 nm, which is consistent with the (002) plane of MoS_2 with hexagonal 2H phase. In addition, the measured interplanar spacing of 0.245 nm corresponds to the (210) plane of CoS_2. The results confirmed that MoS_2 and CoS_2 coexisted in the hybrid structure [21]. Figure 4c and d show the presence and uniform distribution of Mo, S, Co and N in the MOS/COS/CC electrocatalyst.

The chemical composition and valence of elements in MOS/COS/CC-6 h electrocatalyst were studied by XPS. From the XPS spectra of Co in Fig. 5a, it can be seen that the characteristic peaks of Co 2p orbit are deconvoluted into two pairs of spin orbital peaks. The characteristic peaks at 793.4 and 778.2 eV correspond to Co $2p_{1/2}$ and Co $2p_{3/2}$ from Co^{3+}, while the characteristic peaks at 797.5 and 781.4 eV correspond to Co $2p_{1/2}$ and Co $2p_{3/2}$ from Co^{2+}. Two characteristic peaks of Mo 3d were observed at 229.5 and 232.7 eV, corresponding to Mo $3d_{5/2}$ and Mo $3d_{3/2}$ respectively (Fig. 5b), indicating that Mo was in the valence state of +4. The small peak detected at 226.7 eV was attributed to S 2 s orbit. In addition, the S 2 s spectra

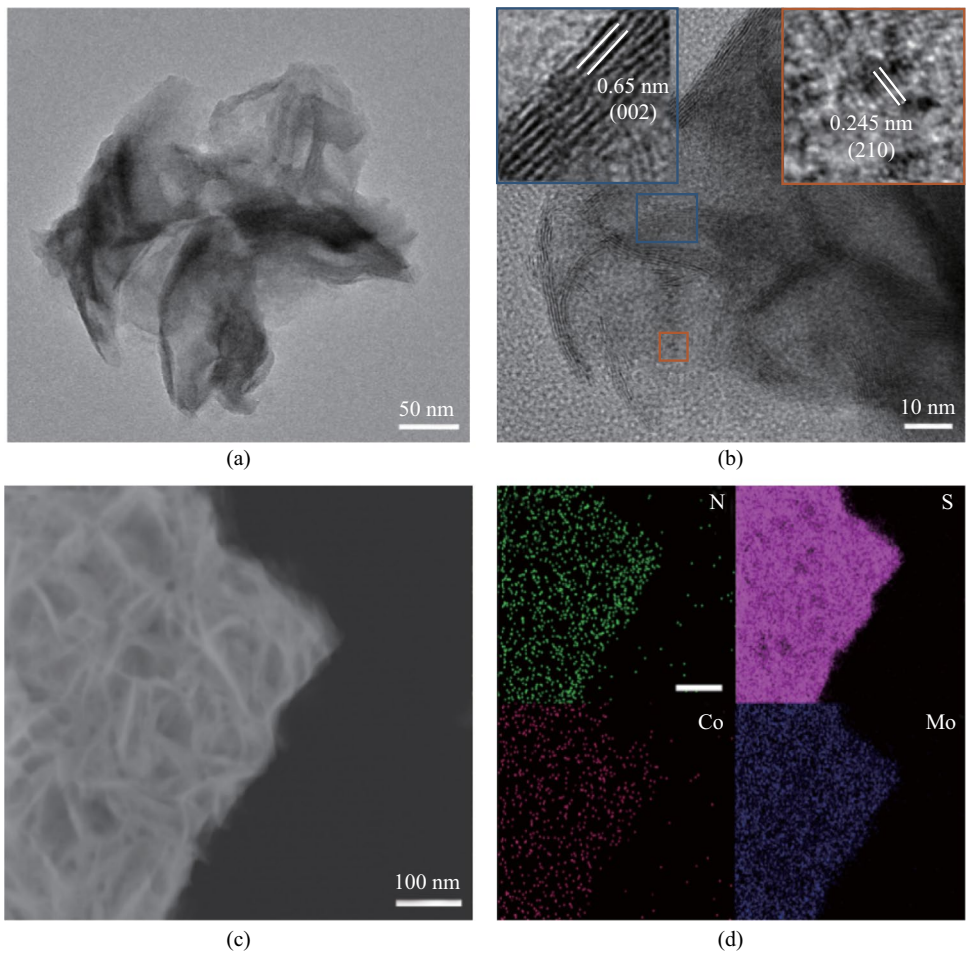

Fig. 4 **a** and **b** TEM images of the MOS/COS/CC-6 h electrocatalyst. Insets are the local HRTEM images. **c** and **d** STEM-EDS elemental maps of N, S, Co and Mo of MOS/COS/CC-6 h

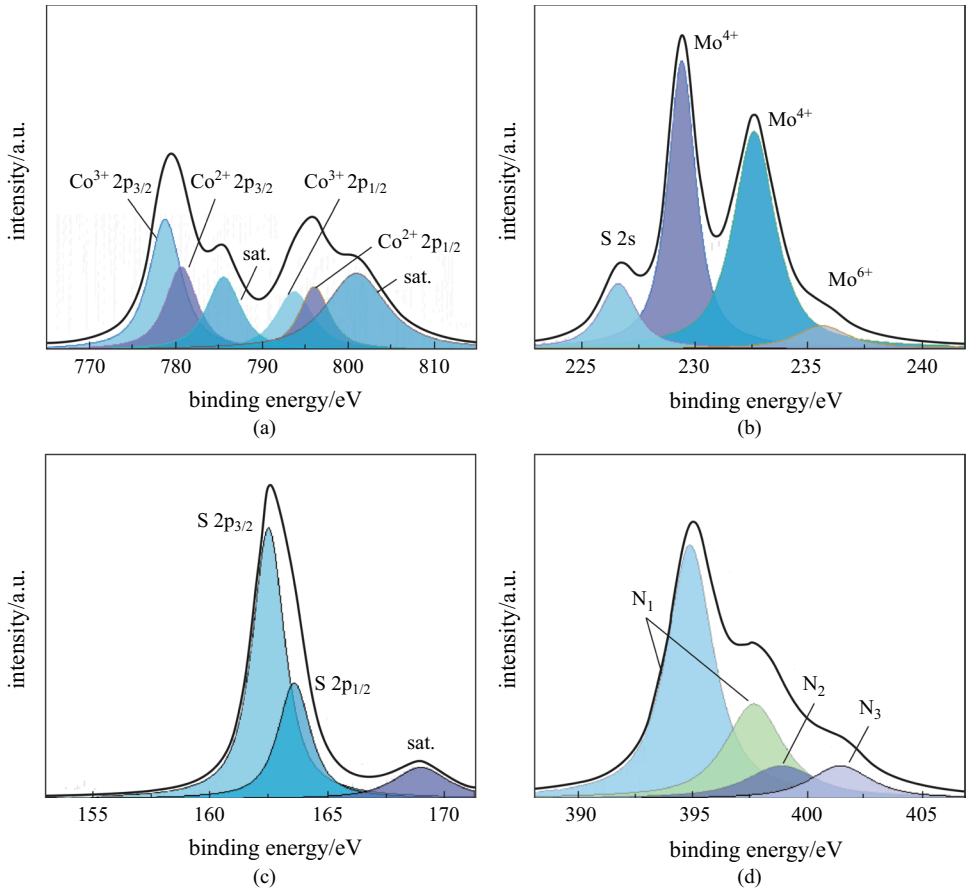

Fig. 5 XPS spectra of MOS/CoS/CC-6 h electrocatalyst. **a** Co, **b** Mo, **c** S, **d** N

could be deconvoluted into two characteristic peaks with binding energies of 226.9 and 227.5 eV, corresponding to the binding energies of S atoms in MoS_2 and CoS_2, respectively. The characteristic peaks of 162.5 and 163.6 eV binding energies in the spectra of S elements belonged to S $2p_{3/2}$ and S $2p_{1/2}$ respectively (Fig. 5c). In the corresponding N 1 s spectrum (Fig. 5d), two characteristic peaks at 395.02 and 397.82 eV were attributed to the Mo–N bond (N_1), while the presence of pyridine N (N_2, 399.03 eV) and graphite N (N_3, 401.57 eV) indicated the successful binding of nitrogen atoms to the carbon substrate [22]. Compared with MOS/COS/CC-4 h and MOS/COS/CC-8 h, the content of Co element in MOS/COS/CC-6 h is in the middle, indicating that with the increase of MoS_2 growth time, the Co element on the material surface gradually decreases (Additional file 1: Fig. S1). In addition, it can be seen from Additional file 1: Fig. S2 that, in the XPS spectrum of the MOS-COS-CC-6 h electrocatalyst, the binding energies of Mo 3d and 2 s shifted compared with those for the Mo element in the MoS_2 electrocatalyst, indicating the interaction between MoS_2 and CoS_2 in the MOS-COS-CC electrocatalyst.

The OER properties of MOS/COS/CC with different growth time and commercial RuO_2 electrocatalysts were tested in 1.0 mol/L KOH. Compared with other electrocatalysts, MOS/COS/CC-6 h only needs an overpotential of 197 mV for a current density of 10 mA/cm^2 (Fig. 6a). The overpotential is significantly lower than that of commercial RuO_2 and other electrocatalysts with different growth times. In addition, the MOS/COS/CC-6 h electrocatalyst had the lowest Tafel slope (64 mV/dec, Fig. 6b), which indicates that it has excellent chemical kinetics for electrocatalytic reaction. Concurrently, we also studied the HER properties of MOS/COS/CC with different growth time and commercial Pt/C electrocatalyst in 1.0 mol/L KOH (Fig. 6c). It can be seen that MOS/COS/CC-6 h and MOS/COS/CC-8 h only required overpotentials of 140 and 125 mV, respectively, to achieve a current density of 10 mA/cm^2. However, the current density of MOS/COS/CC-8 h electrocatalyst decreased greatly at high potential. The reason is that the excessive deposition of MoS_2 nanosheets, which is not conducive to the exposure of active sites and the cracking of the electrocatalyst surface, thus reducing the long-term stability of the electrocatalyst. The catalytic HER kinetics can be estimated

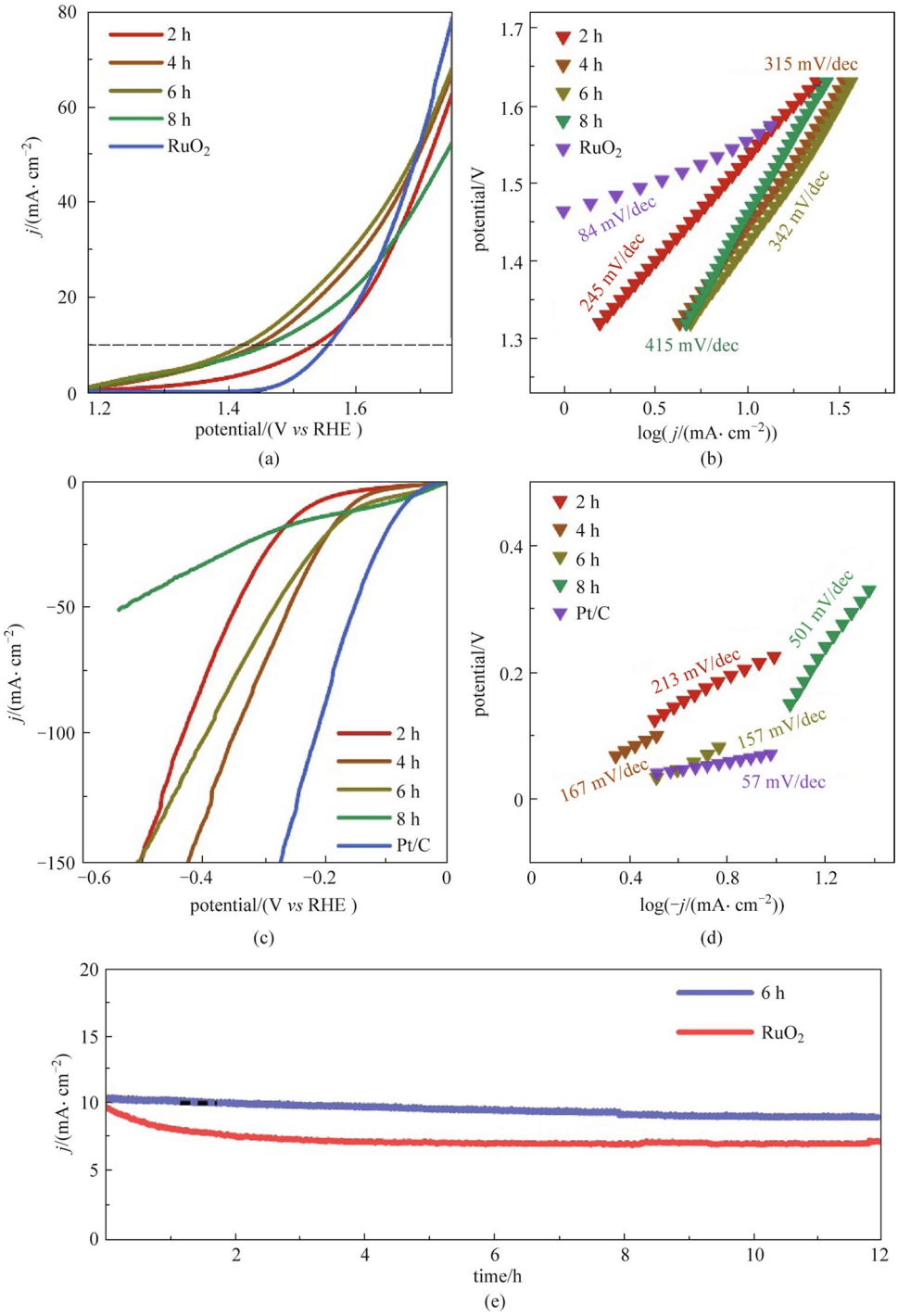

Fig. 6 Electrochemical testing of RuO_2 and MOS/COS/CC electrocatalysts with different synthesis time. **a** LSV curves of OER. **b** Tafel curves of OER. **c** LSV curves of HER. **d** Tafel curves of HER. **e** Stability test of MOS/COS/CC-6 h and RuO_2 electrocatalysts

from the Tafel diagram fitted by the LSV linear curve. As shown in Fig. 6d, the Tafel slope of MOS/COS/CC-6 h is 157 mV/dec, which is smaller than that of MOS/COS/CC-2 h (213 mV/dec) and MOS/COS/CC-8 h (501 mV/dec). This result demonstrates the faster HER catalytic kinetics of MOS/COS/CC-6 h. Furthermore, our material still exhibited relatively excellent catalytic activity in comparison with other bifunctional catalysts (in Table 1).

Besides high catalytic activity, MOS/COS/CC-6 h could also achieve good catalytic stability. As shown in Fig. 6e, the current density decreased by ~ 90% after 12 h reaction, while that of commercial RuO_2 electrocatalyst decreased

Table 1 Comparison of the electrocatalytic performance of MOS/COS/CC with recently reported bifunctional electrocatalysts for water splitting

Catalyst	Water electrolysis test	Current density (j)/($mA \cdot cm^{-2}$)	Overpotential at the corresponding j/mV	Reference
MOS/COS/CC	HER[a]	10	140	This work
	OER[b]	10	194	
Co_5Fe_5-C	HER	10	165	[23]
	OER	10	245	
N-$CoSe_2$@CP	HER	10	106	[24]
	OER	10	237	
$ZnCo_2S_4/CoZn_{13}$	HER	10	160	[25]
	OER	50	274	
Fe-Co-Ni-S_x/NF	HER	10	188	[26]
	OER	10	280	
MoS_2-AB/NF	HER	10	77	[27]
	OER	10	248	
P-$NiSe_2$@N-CNTs/NC	HER	10	95	[28]
	OER	10	206	
10:MoCo-VS_2	HER	10	63	[29]
	OER	10	248	

[a]HER stands for hydrogen evolution reaction

[b]OER stands for oxygen evolution reaction

by 30%. This result indicates that MOS/COS/CC-6 h maintains high structural stability during the test.

4 Conclusions

In conclusion, we have developed a simple and convenient method for constructing hierarchical structure. A bifunctional electrocatalyst with 2D porous N-doped nanosheets embedded with CoS_2 and MoS_2 nanosheets was synthesized by a hydrothermal method. The prepared MOS/COS/CC electrocatalyst showed excellent OER and HER activity in alkaline solution. In OER and HER tests, the MOS/COS/CC-6 h only required overpotentials of 197 and 140 mV at a current density of 10 mA/cm^2 and exhibited lower Tafel slop. These excellent properties are attributed to the abundant active sites and the interaction of MoS_2 and CoS_2 nanosheets. The abundant active sites enable the material to exhibit excellent catalytic activity. Our proposed synthesis strategy can provide an effective tool for realizing high-performance electrocatalysis by exploiting of the synergy between individual nanostructures.

Supplementary Information The online version contains supplementary material available at https://doi.org/10.1007/s12200-022-00034-3.

Acknowledgements This work was financially supported by the National Natural Science Foundation of China (Grant Nos. 51872115 and 52101256), the Open Project Program of Wuhan National Laboratory for Optoelectronics (No. 2018WNLOKF022), the 2020 International Cooperation Project of the Department of Science and Technology of Jilin Province (No. 20200801001GH), Science and Technology Research Project of the Department of Education of Jilin Province (No. JJKH20211083KJ), the Project funded by China Postdoctoral Science Foundation (No. 2020M680043), and the Project supported by State Key Laboratory of Luminescence and Applications (No. KLA-2020-05).

Author contributions XZ carried out data analysis, experimental synthesis and manuscript writing. WZ carried out data analysis and manuscript writing. ZZ carried out data analysis. ZW carried out TEM test and related data analysis. XZ carried out data analysis and manuscript writing. DL carried out data analysis. WZ carried out manuscript writing. All authors read and approved the final manuscript.

Declarations

Competing interests The authors declare that they have no competing interests.

References

1. Chu, K., Liu, Y.P., Li, Y.B., Guo, Y.L., Tian, Y.: Two-dimensional (2D)/2D interface engineering of a MoS_2/C_3N_4 heterostructure for promoted electrocatalytic nitrogen fixation. ACS Appl. Mater. Interfaces **12**(6), 7081–7090 (2020)
2. Luo, Y., Li, X., Cai, X., Zou, X., Kang, F., Cheng, H.M., Liu, B.: Two-dimensional MoS_2 confined $Co(OH)_2$ electrocatalysts for hydrogen evolution in alkaline electrolytes. ACS Nano **12**(5), 4565–4573 (2018)
3. Yang, X., Sun, H., Zan, P., Zhao, L., Lian, J.: Growth of vertically aligned $Co_3S_4/CoMo_2S_4$ ultrathin nanosheets on reduced graphene oxide as a high-performance supercapacitor electrode. J. Mater. Chem. A Mater. Energy Sustain. **4**(48), 18857–18867 (2016)
4. Gao, Y., Xiong, T., Li, Y., Huang, Y., Li, Y., Balogun, M.J.T.: A simple and scalable approach to remarkably boost the overall water splitting activity of stainless steel electrocatalysts. ACS Omega **4**(14), 16130–16138 (2019)
5. Zhao, G., Li, P., Cheng, N., Dou, S.X., Sun, W.: An $Ir/Ni(OH)_2$ heterostructured electrocatalyst for the oxygen evolution reaction: breaking the scaling relation, stabilizing iridium (V), and beyond. Adv. Mater. **32**(24), e2000872 (2020)
6. Xiong, T., Yao, X., Zhu, Z., Xiao, R., Hu, Y.W., Huang, Y., Zhang, S., Balogun, M.J.T.: In situ grown Co-based interstitial compounds: non-3D metal and non-metal dual modulation boosts alkaline and acidic hydrogen electrocatalysis. Small **18**(9), e2105331 (2022)
7. Yang, F., Xiong, T., Huang, P., Zhou, S., Tan, Q., Yang, H., Huang, Y., Balogun, M.S.: Nanostructured transition metal compounds coated 3D porous core-shell carbon fiber as monolith water splitting electrocatalysts: a general strategy. Chem. Eng. J. **423**, 130279 (2021)
8. Wang, Y., Chen, D., Zhang, J., Balogun, M.S., Wang, P., Tong, Y., Huang, Y.: Charge relays via dual carbon-actions on nanostructured $BiVO_4$ for high performance photoelectrochemical water splitting. Adv. Funct. Mater. **32**, 2112738 (2022)
9. Lim, K.J.H., Yilmaz, G., Lim, Y.F., Ho, G.W.: Multi-compositional hierarchical nanostructured $Ni_3S_2@MoS_x$/NiO electrodes for enhanced electrocatalytic hydrogen generation and energy storage. J. Mater. Chem. A Mater. Energy Sustain. **6**(41), 20491–20499 (2018)
10. Zhang, C., Shi, Y., Yu, Y., Du, Y., Zhang, B.: Engineering sulfur defects, atomic thickness, and porous structures into cobalt sulfide nanosheets for efficient electrocatalytic alkaline hydrogen evolution. ACS Catal. **8**(9), 8077–8083 (2018)
11. Wang, X., Zhang, Y., Si, H., Zhang, Q., Wu, J., Gao, L., Wei, X., Sun, Y., Liao, Q., Zhang, Z., Ammarah, K., Gu, L., Kang, Z., Zhang, Y.: Single-atom vacancy defect to trigger high-efficiency hydrogen evolution of MoS_2. J. Am. Chem. Soc. **142**(9), 4298–4308 (2020)
12. Ouyang, T., Wang, X.T., Mai, X.Q., Chen, A.N., Tang, Z.Y., Liu, Z.Q.: Coupling magnetic single-crystal $Co_2Mo_3O_8$ with ultrathin nitrogen-rich carbon layer for oxygen evolution reaction. Angew. Chem. Int. Ed. Engl. **59**(29), 11948–11957 (2020)
13. Zhu, L., Ji, J., Liu, J., Mine, S., Matsuoka, M., Zhang, J., Xing, M.: Designing 3D-MoS_2 sponge as excellent cocatalysts in advanced oxidation processes for pollutant control. Angew. Chem. Int. Ed. Engl. **59**(33), 13968–13976 (2020)
14. Chen, W., Gu, J., Du, Y., Song, F., Bu, F., Li, J., Yuan, Y., Luo, R., Liu, Q., Zhang, D.: Achieving rich and active alkaline hydrogen evolution heterostructures via interface engineering on 2D 1T-MoS_2 quantum sheets. Adv. Funct. Mater. **30**(25), 2000551 (2020)
15. Rui, B., Li, J., Chang, L., Wang, H., Lin, L., Guo, Y., Nie, P.: Engineering MoS_2 nanosheets anchored on metal organic frameworks derived carbon polyhedra for superior lithium and potassium storage. Front. Energy Res. **7**, 142 (2019)
16. Li, Y., Wang, Z., Hu, J., Li, S., Du, Y., Han, X., Xu, P.: Metal–organic frameworks derived interconnected bimetallic metaphosphate nanoarrays for efficient electrocatalytic oxygen evolution. Adv. Funct. Mater. **30**(25), 1910498 (2020)
17. Zhong, H., Luo, Y., He, S., Tang, P., Li, D., Alonso-Vante, N., Feng, Y.: Electrocatalytic cobalt nanoparticles interacting with nitrogen-doped carbon nanotube in situ generated from a metal-organic framework for the oxygen reduction reaction. ACS Appl. Mater. Interfaces **9**(3), 2541–2549 (2017)
18. Hu, L., Hu, Y., Liu, R., Mao, Y., Balogun, M.S., Tong, Y.: Co-based MOF-derived $Co/CoN/Co_2P$ ternary composite embedded in N- and P-doped carbon as bifunctional nanocatalysts for efficient overall water splitting. Int. J. Hydrogen Energy **44**(23), 11402–11410 (2019)
19. Yilmaz, G., Yang, T., Du, Y., Yu, X., Feng, Y.P., Shen, L., Ho, G.W.: Stimulated electrocatalytic hydrogen evolution activity of MOF-derived MoS_2 basal domains via charge injection through surface functionalization and heteroatom doping. Adv. Sci. (Weinh.) **6**(15), 1900140 (2019)
20. Zhou, J., Dou, Y., Zhou, A., Guo, R.M., Zhao, M.J., Li, J.R.: MOF template-directed fabrication of hierarchically structured electrocatalysts for efficient oxygen evolution reaction. Adv. Energy Mater. **7**(12), 1602643 (2017)
21. Chen, Z., Ha, Y., Jia, H., Yan, X., Chen, M., Liu, M., Wu, R.: Oriented transformation of Co-LDH into 2D/3D ZIF-67 to achieve Co–N–C hybrids for efficient overall water splitting. Adv. Energy Mater. **9**(19), 1803918 (2019)
22. Guo, Y., Tang, J., Henzie, J., Jiang, B., Xia, W., Chen, T., Bando, Y., Kang, Y.M., Hossain, M.S.A., Sugahara, Y., Yamauchi, Y.: Mesoporous iron-doped $MoS_2/CoMo_2S_4$ heterostructures through organic-metal cooperative interactions on spherical micelles for electrochemical water splitting. ACS Nano **14**(4), 4141–4152 (2020)
23. Yan, Y., Han, Y., Wang, F., Hu, Y., Shi, Q., Diao, G., Chen, M.: Bifunctional electrocatalyst of Co_xFe_y-C for overall water splitting. J. Alloys Compd. **897**, 163126 (2022)
24. Wei, G., Xu, Z., Zhao, X., Wang, S., Kong, F., An, C.: N-doped $CoSe_2$ nanomeshes as highly-efficient bifunctional electrocatalysts for water splitting. J. Alloys Compd. **893**, 162328 (2022)
25. Zhao, D., Dai, M., Liu, H., Duan, Z., Tan, X., Wu, X.: Bifunctional $ZnCo_2S_4@CoZn_{13}$ hybrid electrocatalysts for high efficient overall water splitting. J. Energy Chem. **69**, 292–300 (2022)
26. Zhu, S., Lei, J., Wu, S., Liu, L., Chen, T., Yuan, Y., Ding, C.: Construction of Fe-Co-Ni-S_x/NF nanomaterial as bifunctional electrocatalysts for water splitting. Mater. Lett. **311**, 131549 (2022)
27. Guo, L., Liu, Q., Liu, Y., Chen, Z., Jiang, Y., Jin, H., Zhou, T., Yang, J., Liu, Y.: Self-supported tremella-like MoS_2-AB particles on nickel foam as bifunctional electrocatalysts for overall water splitting. Nano Energy **92**, 106707 (2022)
28. Yu, J., Li, W.J., Kao, G., Xu, C.Y., Chen, R., Liu, Q., Liu, J., Zhang, H., Wang, J.: *In-situ* growth of CNTs encapsulating P-doped $NiSe_2$ nanoparticles on carbon framework as efficient bifunctional electrocatalyst for overall water splitting. J. Energy Chem. **60**, 111–120 (2021)
29. Singh, V.K., Nakate, U.T., Bhuyan, P., Chen, J., Tran, D.T., Park, S.: Mo/Co doped 1T-VS_2 nanostructures as a superior bifunctional electrocatalyst for overall water splitting in alkaline media. J. Mater. Chem. A Mater. Energy Sustain. **10**(16), 9067–9079 (2022)

Xingwei Zhou received his master degree in School of Materials Science and Engineering, Jilin University, China in 2021. Now he is a process engineer at Intel-Dalian. His current research interest is the production process of 3D NAND semiconductor products and optimization/improvement of relevant processes.

Wei Zhang obtained his Ph.D. degree from Institute of Metal Research Chinese Academy of Sciences, China in 2004. Then he held positions in NIMS-Japan, Samsung AIT-Republic of Korea, Fritz-Haber Institute of MPG-Germany, DTU-Denmark and CIC Energigune-Spain. He was awarded *Ikerbasque Research Professor* in 2016. In 2014, he became a full professor at Jilin University, China and has been selected as *Tang Auchin Scholar – Leading Professor* since 2020; Now he serves as the Director of the Electron Microscopy Center of Jilin University. His current research focuses on surface and interface of advanced energy materials and catalysts.

Zunhao Zhang received her master degree in College of Life Sciences, Jilin University, China in 2018. Now she is a laboratory technician at Electron Microscopy Center, Jilin University. Her current research interest is analysis of materials surface.

Zizhun Wang received his degree of master degree in College of Food Science and Engineering, Jilin University, China in 2018. Now she is a laboratory technician at Electron Microscopy Center, Jilin University. His current research interests include transmission electron microscopy and energy dispersive X-ray spectroscopy analysis.

Xu Zou is a postdoc at School of Materials Science and Engineering, Jilin University, China. She received her Ph.D. degree in 2020 from State Key Laboratory of Inorganic Synthesis and Preparative Chemistry, College of Chemistry, Jilin University, China. Her current research focuses on design and structure–activity relationship of electrocatalytic water splitting materials.

Dabing Li obtained his Ph.D. degree from Institute of Semiconductor, Chinese Academy of Sciences, China in 2004. Then he held positions in Mie University-Japan from 2004 to 2007. Then he worked in State Key Laboratory of Luminescence and Applications, Changchun Institute of Optics, Fine Mechanics and Physics, Chinese Academy of Sciences, and he is now a distinguished professor. His current research focuses on GaN-based and other luminescence materials and devices.

Weitao Zheng is Professor and Vice President of Jilin University, China. He obtained his Ph.D. degree from Jilin University in 1990. After that, he held positions at the Royal Institute of Sweden, Linköping University, Chiba Institute of Technology, and Nanyang University of Technology. His current research focuses on energy materials, functional thin films, and catalysts.